JACS
JOURNAL OF THE AMERICAN CHEMICAL SOCIETY

ARTICLE

pubs.acs.org/JACS

Sources of Conductivity and Doping Limits in CdO from Hybrid Density Functional Theory

Mario Burbano, David O. Scanlon,* and Graeme W. Watson*

School of Chemistry and CRANN, Trinity College Dublin, Dublin 2, Ireland

ABSTRACT: CdO has been studied for decades as a prototypical wide band gap transparent conducting oxide with excellent *n*-type ability. Despite this, uncertainty remains over the source of conductivity in CdO and over the lack of *p*-type CdO, despite its valence band maximum (VBM) being high with respect to other wide band gap oxides. In this article, we use screened hybrid DFT to study intrinsic defects and hydrogen impurities in CdO and identify for the first time the source of charge carriers in this system. We explain why the oxygen vacancy in CdO acts as a shallow donor and does not display negative-*U* behavior similar to all other wide band gap *n*-type oxides. We also demonstrate that *p*-type CdO is not achievable, as *n*-type defects dominate under all growth conditions. Lastly, we estimate theoretical doping limits and explain why CdO can be made transparent by a large Moss−Burstein shift caused by suitable *n*-type doping.

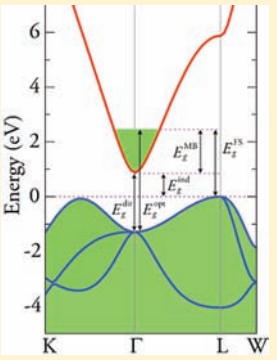

INTRODUCTION

Transparent conducting oxides (TCOs) are compounds which combine the normally mutually exclusive properties of transparency and conductivity. Most highly transparent materials, such as glass, behave as insulators with high electrical resistivities of $>10^{10}$ Ω cm, whereas materials with low resistivities (10^{-4}−10^{-7} Ω cm), such as metals, do not transmit visible light. The combination of both properties in a single material is thus quite an unusual phenomenon, and TCOs have proved indispensable in the development of optoelectronic devices such as solar cells, flat panel displays, and light emitting diodes.[1−4] At present, the current industry standard *n*-type TCO is In_2O_3:Sn (ITO) which usually demonstrates conductivities of $\sim 10^4$ S cm^{-1} while retaining >90% transparency.[5] The overwhelming demand for ITO, coupled with the low abundance of indium within the earth's crust, has made indium an increasingly expensive commodity, however, which has led to a large research drive to replace ITO as the industry standard TCO.[6]

Rocksalt (RS) structured CdO is an *n*-type degenerate semiconductor which possesses a small indirect band gap (E_g^{ind}) of ∼0.84 eV[7] and a larger direct band gap (E_g^{dir}) of ∼2.2 eV.[8,9] CdO is a highly nonstoichiometric material and generally possesses large carrier concentrations ($\sim 10^{18}$−10^{20} cm^{-3}) together with large electron mobilities in the bulk.[10] These high carrier concentrations generate a pronounced Moss−Burstein (MB) shift which can considerably extend the optical band gap, E_g^{opt}.[11] Donor dopants can extend E_g^{opt} above 3.1 eV, making CdO suitable for TCO applications. Mobilities of the order of ∼200 cm^2 V^{-1} s^{-1} and conductivities as high as 42 000 S cm^{-1} have been reported for doped CdO samples,[12] which is an order of magnitude higher than the typical conductivities of the industry standard TCOs. Understanding the defect chemistry of CdO is therefore vital for the development of improved TCOs.

To date, however, there is still uncertainty regarding the nature of the dominant intrinsic defects in this material. Cd interstitials (Cd_i)[13,4] and oxygen vacancies (V_O)[15,16] have both been suggested as the dominant defects in CdO. Similar to other *n*-type TCOs,[17] hydrogen impurities have also been suggested both experimentally[18] and theoretically[19] to act as donors in CdO. A recent experimental study by King et al. found that intrinsic defects and H impurities *all* act as shallow donors in CdO.[20] This finding is intriguing, as in all other *n*-type TCOs V_O acts as a *deep* donor, and cation interstitials (while being shallow donors) are generally too high in energy to contribute heavily toward any intrinsic conductivity.[21,22] This suggests that intrinsic defects behave differently in CdO compared to the other TCOs. Surprisingly, a full ab initio defect analysis of CdO to clarify this behavior has not been undertaken thus far.

In this study, we examine the formation of intrinsic defects and hydrogen impurities in CdO using screened hybrid density functional theory (h-DFT). We demonstate (i) that V_O is the dominant intrinsic defect in CdO, acting as a doubly ionized shallow donor, (ii) that hydrogen defects also act as shallow donors in CdO and dominate under Cd-poor/O-rich conditions, (iii) that *p*-type conductivity can never be realized in CdO, despite it possessing a suitably high VBM, and (iv) why large MB shifts are achievable in doped CdO.

RESULTS

The calculated lattice parameters, bond lengths, and electronic structure data for PBE and h-DFT (PBE and HSE06 functionals; calculation details in Methods section) calculated CdO are presented in Table 1. The HSE06 structure is only slightly

Received: May 20, 2011
Published: August 19, 2011

dx.doi.org/10.1021/ja204639y | *J. Am. Chem. Soc.* 2011, 133, 15065–15072

Table 1. Geometrical and Electronic Structure Data for CdO Calculated Using GGA-PW91, GGA-PBE, and HSE06 and Compared to Known Experiments[a]

	GGA-PW91[24]	GGA-PBE (this study)	HSE06 (this study)	exptl
a	4.80	4.79	4.72	4.70[23]
d_{Cd-O}	–	2.39	2.36	2.35[23]
volume	110.59	109.90	105.15	103.82[23]
E_g^{dir}	0.60	0.61	2.18	2.16–2.20[8,9]
E_g^{ind}	−0.51	−0.51	0.89	0.84–0.90[27]
VB width	∼4.00	3.94	4.45	∼5.00[28]
d states	∼−6.60	−5.7 to −7.4	−6.5 to −8.3	∼−8.50[26]

[a] a is the lattice parameter, measured in Å; d_{Cd-O} is the Cd−O bond length in Å; the volume is measured in Å^3; E_g^{dir} is the direct band gap in eV; E_g^{ind} is the indirect band gap in eV; VB width is the width of the main valence band in eV; and d states is the position of the Cd d states relative to the VBM at 0 eV and is measured in eV.

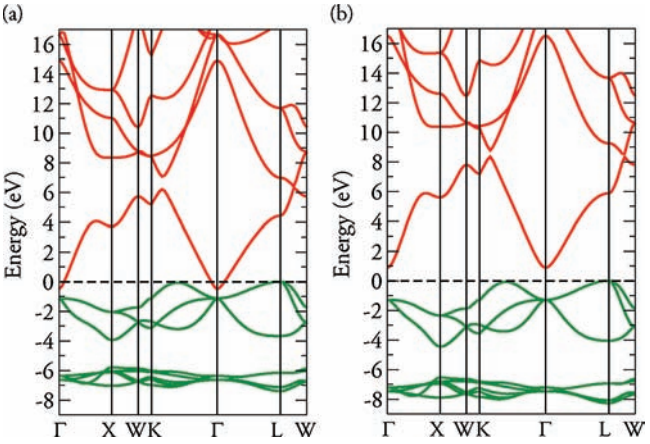

Figure 1. (a) PBE and (b) HSE06 calculated band structure for CdO. The VBM is set to 0 eV in both cases and is denoted by a horizontal dashed black line. Green and red bands denote valence and conduction bands, respectively. Note how the PBE calculated conduction band comes down below the VBM, indicating a semimetallic system.

overestimated with respect to the experimental values[23] and is more accurate than standard DFT functionals.[24] HSE06 has previously been shown to be better at accurately predicting the structure and band gap data of many semiconductors compared to standard DFT functionals. In fact, it has been shown that standard DFT functionals are not able to accurately calculate the band structure features of CdO, even predicting CdO to be a semimetal,[24] and that methods that go beyond GGA/LDA must be employed.[25,26] Both the PBE and the HSE06 calculated band structure for CdO are shown in Figure 1. The valence band maximum (VBM) occurs at L, which is slightly higher than the Σ line (between K and Γ). PBE yields a band structure in which the CBM comes down below the VBM, indicating a semimetallic system, which agrees with previous standard DFT results.[25,26]

From the HSE06 band structure (Figure 1(b)), we obtain values of 2.18 and 0.89 eV for E_g^{dir} and E_g^{ind}, respectively. These results compare well with recent experimental studies which reported E_g^{dir} to be 2.20[9] and 2.16 eV.[8] The most recent measurement of the E_g^{ind} (0.90 eV)[27] is also in excellent agreement with our HSE06 calculated E_g^{ind}. For an effective TCO material, it is important that the second conduction band (CBM+ 1) is separated from the CBM by greater than 3.1 eV.[29] This large CBM−CBM+ 1 separation ensures that any donor electrons in the conduction band are not excited by visible light to the next conduction band and therefore ensures optical transparency, which is vital for device performance. Similarly, for *p*-type TCOs, absorption must not occur from bands within ∼3.1 eV of the VBM to the holes states near the VBM.[30,31] For CdO, the CBM+ 1 is ∼15 eV higher than the CBM, indicating that the conduction band features of CdO are ideal for a candidate TCO.

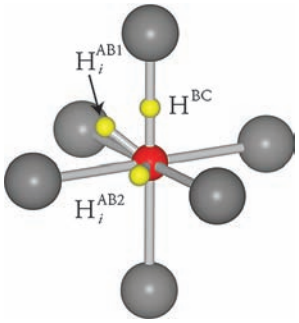

Figure 2. Positions of hydrogen intersitials in CdO: diagonal (H_i^{AB1}), facial hydrogen (H_i^{AB2}), and bond centered hydrogen (H^{BC}). Cd, O, and H are denoted by gray, red, and yellow spheres, respectively.

Our HSE06 calculated effective mass for the CBM is 0.21 m_e and for the VBM is 1.3 m_e. To the best of our knowledge, the valence band effective masses have never been measured experimentally; however, our conduction band effective mass is in good agreement with the most recent experimental measurements of the effective mass (0.21 m_e and 0.24 m_e).[8,9] The experimental valence bandwidth of CdO is ∼5 eV,[28] which agrees well with our calculated VB width of ∼4.5 eV. Overall, the HSE06 functional describes the electronic structure features of CdO much better than standard functionals and yields results in excellent agreement with experiments and also in good agreement with the results of the computationally intensive, higher-level GW quasiparticle calculations of Bechstedt and co-workers.[32]

Defect Energetics and Transition Levels. The defects considered in this study include *n*-type V_O and Cd_i as well as the *p*-type oxygen interstitial (O_i) and cadmium vacancy (V_{Cd}). In addition, H was incorporated in a number of lattice positions, namely, hydrogen in an oxygen lattice site (H_O) and four different interstitial positions. The intersitial positions tested were the perfect interstitial site, anion antibonding sites 1 Å from an O along the ⟨111⟩ direction (H_i^{AB1}), the ⟨110⟩ direction (H_i^{AB2}), and the bond centered site (H^{BC}, as illustrated in Figure 2.

A plot of formation energy as a function of Fermi-level position for all intrinsic defects and H-related impurities for both Cd-*rich*/O-*poor* and Cd-*poor*/O-*rich* regimes is displayed in Figure 3. For the intrinsic *n*-type defects, it is clear that the V_O is the most stable defect under both sets of conditions and will dominate intrinsic conductivity. The Cd_i, which had previously been suggested as the dominant defect,[13,14] is considerably higher in energy and is unlikely to play a large role in conductivity in CdO. The low formation energies of the V_O under both growth conditions can explain the observed nonstoichiometry of CdO samples.[10] Both V_O and Cd_i exist only in the +2 charge state in the band gap, which is consistent with previous experimental studies which reported that the source of undoped charge carriers in CdO was doubly ionized donors.[20] Interestingly, CdO represents the only

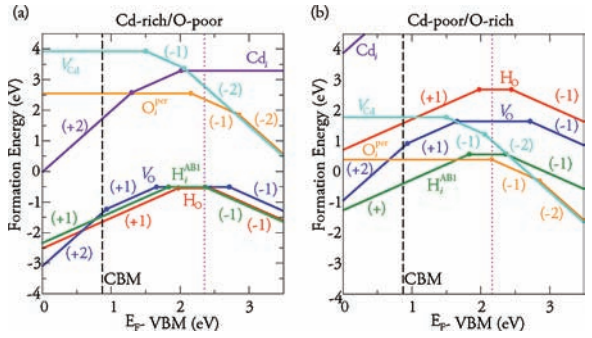

Figure 3. Formation energies for intrinsic and hydrogen defects under (a) Cd-rich/O-poor conditions and (b) Cd-poor/O-rich conditions. The solid dots represent the transition levels $\varepsilon(q/q')$. The black dashed line indicates the position of the conduction band maximum (CBM), with the purple vertical dotted line representing the maximum achievable Fermi level before compensation occurs.

wide band gap *n*-type TCO in which V_O acts as a shallow donor. In ZnO,[21] SnO_2,[22] Ga_2O_3,[33] and In_2O_3,[34] V_O has been found to be a deep donor, with "undoped" conductivity thought to arise from the presence of adventitious hydrogen.[17,22,35,36]

The lowest energy H impurity in CdO under Cd-*rich*/O-*poor* conditions is H_O, which is slightly more stable than H_i^{AB1}, with both defects being lower in energy than V_O as the Fermi level is raised to the CBM and beyond. Both H on the perfect interstitial site and H_i^{AB2} were found to relax to the H_i^{AB1} position. Under Cd-*poor*/O-*rich* conditions, H_i^{AB1} is the most stable defect considered and will dominate conductivity. The H defects are all in the +1 charge state in the gap, indicating that H behaves exclusively as a shallow donor in CdO. Shallow donor behavior of H_i and H_O has been noted previously for other wide band gap *n*-type oxides.[17,22,35−38] Our results agree closely with those of King et al. who found that native defects and hydrogen impurities *both* act as shallow donors in CdO samples.[20]

***p*-Type CdO?** Recent valence band alignments for wide band gap oxides have indicated that the VBM of CdO is quite high compared to the other wide band gap TCOs.[39,40] By the doping limit rules,[41] this indicates that the VBM of CdO lies in the "*p*-dopable range" and indicates the possibility of CdO being a bipolar material, which would be very much sought after for the development of functional TCO *p*−*n* junctions. To the best of our knowledge, however, no reports of *p*-type CdO have ever been published. To investigate the possibility of *p*-type CdO, we now analyze the formation of O_i and V_{Cd}. We started our O_i calculations with the O positioned on the perfect interstitial site; however, the O moved toward one of the lattice oxygens, displacing it from its lattice site and forming a peroxide (O−O dumbell-like) species, as shown in Figure 4, which we will now denote as O_i^{per}. This type of behavior has also been noted for ZnO,[42,43] Al_2O_3,[44] and SnO_2.[45,46] It is instructive to note that the structure of O_i^{per} is very similar to the structure of the anions in CdO_2, which has an RS-like structure with peroxide anions, O_2^{2-}, on the regular RS anion sites.[47] Our calculations reveal that this O_i^{per} is the most stable *p*-type defect under both growth conditions; however, it is higher in energy than the lowest *n*-type defects under both sets of conditions. Both Cd_i and the O_i^{per} exist only in the neutral charge state over the range of the band gap, under both sets of conditions, indicating that they will not act as effective acceptors in this system. These findings explain why *p*-type CdO samples are never reported, despite it possessing a relatively high VBM.

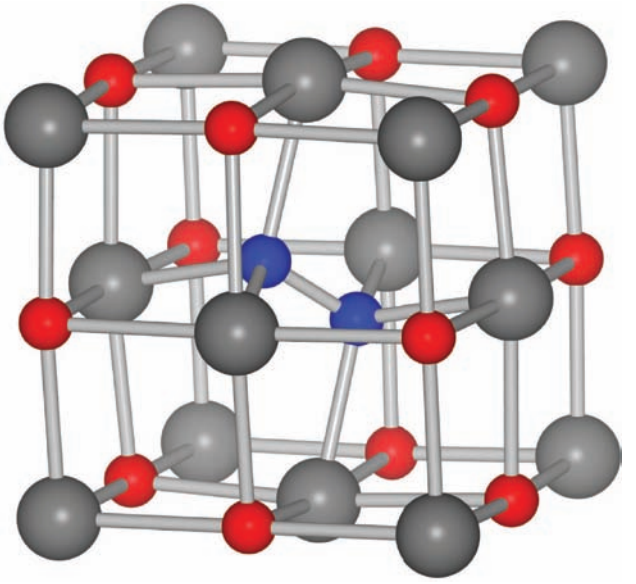

Figure 4. Converged structure of an oxygen peroxide, O_i^{per}, in the CdO lattice. The two blue spheres denote the O−O dumbell.

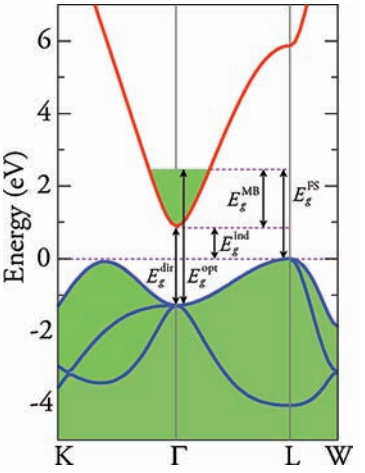

Figure 5. Schematic band structure highlighting the Fermi level stabilization energy, E_g^{FS}, the Moss−Burnstein shift, E_g^{MB}, and the optical band gap, E_g^{opt}, for defective CdO. The green shaded areas indicate occupation by electrons. The VBM is set to 0 eV.

Doping Limits. Under both sets of growth conditions, compensation by *p*-type defects is not expected to occur until well above the CBM, as indicated by the vertical dotted line in Figure 3(a) and (b). This limit can be taken as an approximation of the Fermi level stabilization energy, E_g^{FS}, which is the Fermi level at which the formation energy of donor defects and acceptor defects is equal.[48] The definition of E_g^{FS} is based on the amphoteric defect model proposed by Walukiewicz[48] and means that for Fermi levels above (below) E_g^{FS} acceptor (donor) defects are favored.[49] Our computed transition levels only represent a first approximation to the doping limits, as they ignore the effects of band gap renormalization, changes to the parabolicity of the CBM as the number of charge carriers increases,[50] and the effect of electron accumulation layers on the band gap.[51] Nevertheless, the results can be used to rationalize the doping behavior seen experimentally. Taking the Cd-poor/O-rich conditions, our predicted *maximum* Fermi level

position above the VBM before compensation can occur is 2.15 eV (also indicated by E_g^{FS} in Figure 5), which implies a maximum Moss−Burstein shift (E_g^{MB}) of the order of 1.26 eV. Similarly for Cd-rich/O-poor, we obtain an E_g^{MB} of 1.43 eV, with the true MB shift expected to lie in between the two extremes. These values are in good agreement with the Fermi level positions reported by Piper et al. (∼1.15 and ∼1.30 eV),[52,53] and Speaks et al. (∼1.00 eV).[49] This in turn implies *optical* band gaps, E_g^{opt}, of between ∼3.44 and ∼3.61 eV. Experimentally, donor doping of CdO has produced widespread optical band gaps,[11,54,55] ranging from the direct band gap of 2.18 eV to the highest reported band gap of 3.38 eV for CdO:Sc.[55]

Using our calculated maximum Moss−Burstein shift and our calculated effective mass of the CBM, we can estimate the number of charge carriers in doped CdO from free electron theory using

$$E_{BM} = \frac{\hbar^2}{2m^*}(3\pi^2 n_e)^{2/3} \quad (1)$$

where m^* is derived from the valence and conduction band effective masses, m_V and m_C according to $(1/m^*) = (1/m_C) + (1/m_V)$, and n_e is the electron carrier concentration. On the basis of our approximate model, this analysis predicts the maximum carrier concentration to be ∼4.34×10^{20} and ∼5.25×10^{20} cm^{-3} for Cd-poor/O-rich and Cd-rich/O-poor conditions, respectively, before compensation by *p*-type defects occurs. These numbers agree quite well with the saturation carrier concentration reported for CdO (at the E_g^{FS}), which was ∼5×10^{20} cm^{-3}.[49]

DISCUSSION

Our h-DFT calculations have shown that the formation energy of V_O is much lower than that of the Cd_i under all growth conditions, indicating that previous studies which identified Cd_i as the dominant defect[13,14] were misguided. The low formation energy of V_O explains the fact that CdO samples are often found to be highly substoichiometric.[10] Both V_O and Cd_i are found to act as shallow donors in CdO, meaning that the behavior of V_O in CdO is very different from that reported for V_O in other wide band gap *n*-type TCOs, i.e., ZnO,[56−59] SnO_2,[60] Ga_2O_3,[33] and In_2O_3.[36,60] In these *n*-type TCOs, V_O is found be stable only in the 0 and +2 charge states, meaning it is a negative-*U* defect. In CdO however, V_O is stable only as +2 in the band gap and does not display any negative-*U* character.

The origin of this can be understood by examining the structure of the V_O in the 0, +1, and +2 charge states. For the 0 (neutral) charge state, the Cd ions neighboring the vacancy move outward from the vacancy by 1.7%, with the nearest-neighbor oxygen moving toward the vacancy by 1.1% relative to the bulk bond lengths. For the +1 charge state, the Cd ions move a further 1.4%, and the oxygen moves toward the vacancy by a further 0.5%. This trend is continued for the +2 charge state, with the Cd moving away from the vacancy by a further 1.4% and the O moving inward by another 0.5%. These small relaxations are in stark contrast to the large relaxations experienced by, for example, V_O in ZnO,[57,58,61] which has been shown to experience a 12% relaxation of the four Zn ions neighboring a vacancy *toward* the vacancy site. For the +1 and +2 charge, the Zn ions then relax away from the vacancy by 2% and 23%, respectively, and it is the large relaxations experienced by the 0 and +2 charge states which stabilize these charge states relative to the +1 charge state, making the V_O a negative-*U* center in ZnO. As V_O in CdO does not experience any large lattice distortions, there is no driving force for negative-*U* behavior.

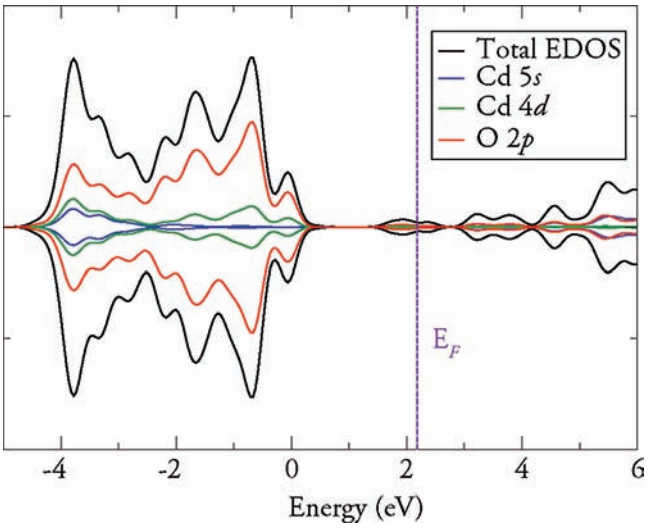

Figure 6. Partial density of states for V_O in the 64 atom CdO supercell. The position of the Fermi level, E_F, is indicated by the purple vertical dashed line. The VBM is set to 0 eV. The denisty of states includes a Gaussian smearing of 0.2 eV.

At this point it is instructive to think about an oxygen vacancy in Kroger−Vink notation, i.e., $[V_O^{\bullet\bullet} + 2e]$, which means that there is a doubly positive vacancy on an oxygen site, plus two free electrons. The doubly positive vacancy would be expected to *repel* the neighboring positively charged cations; however, for ZnO the cations move toward the vacancy,[57,61] indicating that there is significant negative charge in the vacancy site. This is explained by the fact that electrons are trapped in the V_O, in an F-center-like fashion in ZnO, complete with polaronic distortion.[58] For the V_O^{+2} in ZnO, the two electrons are now absent from the vacancy, and the Zn ions are strongly repelled away from the vacancy site. The reason that V_O behaves differently in CdO can also be rationalized by considering the nature of the electrons left behind up on V_O formation. Bader[62] analysis of these two electrons shows that only 0.46 of an electron is present in the vacancy position, with the other 1.54 electrons delocalized over the Cd and O ions neighboring the vacancy. This is noticeably less localized than the electrons in the ZnO V_O.[21,58] The origin of the negative-*U* behavior in other wide band gap *n*-type TCOs, therefore, is the trapping of the electrons in the vacancy position, and this does not occur in the case of CdO. This type of delocalization behavior in CdO is more in keeping with V_O being a shallow donor rather than a deep donor. Similarly, the single particle levels (raw eigenvalues of the defects states) for the V_O lie in the bottom of the conduction band in CdO. This is illustrated in Figure 6, which shows that the Fermi energy is resonant in the conduction band upon V_O formation, with no defect states in the band gap, which is at variance with the deep V_O single particle levels in ZnO, SnO_2, Ga_2O_3, and In_2O_3.[21,33,36,56−60] To the best of our knowledge, this type of shallow donor behavior of V_O in wide band gap oxides has only been reported for one other oxide, Tl_2O_3,[63] which possesses a small fundamental band gap of ∼0.33 eV and a much larger optical band gap of >2.3 eV.

We find that H-related impurities also have very low formation energies in CdO under all growth conditions and will always act as shallow donors. For O-*poor*/Cd-*rich* conditions, *n*-type conductivity in the system will be controlled by the concentration of

V_O, H_O, and H_i^{AB1}, with H_O slightly more favored at higher E_F. Under Cd-*poor*/O-*rich* conditions, H_i^{AB1} is the dominant defect, meaning that any H in the growth environment will cause unintentional *n*-type conductivity under all growth conditions. These findings are in good agreement with the recent experiments of King et al. who found that both intrinsic defects *and* H-related impurities act as shallow donors in CdO.[20]

According to the doping limit rules,[41,48,64−67] the higher a material's VBM is on an absolute scale, the easier it is to dope the material and make it *p*-type. This should also mean that native *p*-type defects *should* have reasonably low formation energies under Cd-*poor*/O-*rich* growth conditions relative to the native *n*-type defects. Although CdO possesses a high VBM relative to other oxide materials,[39,40] it also possesses a low CBM relative to other oxides, due to its low indirect band gap.[39,40] Hosono and co-workers have recently championed SnO as a possible bipolar material, listing small indirect/forbidden band gaps coupled with larger optical band gaps as the key factors in finding good candidate bipolar semiconductors.[68] By these standards, CdO should represent a very strong candidate for bipolar activity. Our calculations, however, indicate that even though the O_i^{per} has the lowest *neutral* formation energy of the native acceptor defect in CdO under Cd-*poor*/O-*rich* conditions the acceptor ionization levels for this material are deep in the conduction band, indicating that it cannot act as an effective acceptor in CdO. For E_F close to the valence band maximum (which should be optimal for *p*-type defects), H_i^{AB1} and V_O^{+2} are both lower in energy and will always compensate the native acceptors. Therefore, despite possessing a high VBM, CdO can never show *p*-type conductivity from intrinsic defects, and it is unlikely that extrinsic acceptors could cause *p*-type conductivity due to the very low formation energies of the *n*-type defects. Our calculations indicate that although a high VBM relative to the vacuum is a good indicator of *p*-type ability the ultimate behavior is determined by the defect chemistry. In this respect, high level *ab initio* calculations can prove invaluable.

Lastly, we addressed the doping limits of CdO, using the 0/−1 ionization levels of all the defects considered to approximate the point where compensation by acceptors or electron trapping occurs. Our calculations indicate that the point where compensation occurs, which can be likened to the Fermi stabilization energy, E_g^{FS} (also known as the charge neutrality level or alternatively the branch point energy[69,70]), is situated deep in the conduction band, with calculated limits of 1.26−1.43 eV above the CBM depending on the growth conditions. These approximate limits agree quite well with recent experiments that list the E_g^{FS} for CdO to be ∼1.15,[52] ∼1.00,[49] and ∼1.30 eV.[53] The distance of the E_g^{FS} above the CBM represents the Moss−Burstein shift possible in doped CdO, before compensation occurs, and our limits agree well with the large optical band gaps seen experimentally.[11,54,55,71−76] Our study therefore demonstrates that the large charge carrier concentrations and big optical band gaps of CdO are allowed by the fact that *n*-type defects are not compensated by *p*-type defects until deep in the conduction band.

This type of uncompensated *n*-type defect chemistry behavior is also seen for other materials (e.g., InN[77−83] and InAs[84−86]) where very large carrier concentrations are sustainable. For In_2O_3, the E_g^{FS} has been reported to be in the range 0.30−0.65 eV above the CBM.[87,88] If you take into account that the effective mass for CdO is reported to be less than or comparable to that of In_2O_3,[89] and use eq 1, then it is clear that CdO can sustain a much higher carrier concentration than In_2O_3. This is the vital factor in doped CdO producing the highest conductivities of any TCO reported previously.[12] To move the field of TCOs forward, alternatives to the expensive and rare In_2O_3 and the toxic CdO must be found. This could be achieved by devising strategies to raise the E_g^{FS} of the abundant TCOs such as SnO_2 or ZnO (or alternatively lower the CBM of these materials) while retaining the same characteristic conduction band dispersion and maintaining optical transparency. Whatever strategies may emerge, the defect chemistry of CdO provides a glimpse of the ideal defect chemistry of a candidate TCO and should serve as a guide to the experimentalists and theoreticians alike in the search for novel TCOs.

CONCLUSION

We have revealed that V_O is the dominant intrinsic defect in CdO under all growth conditions, acting as a doubly ionized shallow donor. Conductivity in nominally "undoped" CdO is likely to be dominated by V_O and H impurities under all growth conditions. Despite the relatively high VBM of CdO, *p*-type CdO will never be realized as the formation energy of the *p*-type defects is too high in energy; their ionization levels are ultra deep; and they are always compensated by *n*-type defects. We have examined the doping limits of CdO and find that compensation by *p*-type defects does not occur until >1.2 eV above the CBM, explaining why the band gap of CdO can experience large Moss−Burstein shifts which can extend the optical band gap from ∼2.2 eV to a reported ∼3.4 eV.

METHODS

All calculations were performed using the periodic DFT code VASP,[90,91] in which a plane-wave basis set describes the valence electronic states. The Perdew−Burke−Ernzerhof[92] (PBE) gradient corrected functional was used to treat the exchange and correlation. The projector-augmented wave[93,94] (PAW) method was used to describe the interactions between the cores (Cd:[Kr] and O:[He]) and the valence electrons. In this way, the Cd 4d states are explicitly included in the valence. To counteract the self-interaction error and the band gap errors inherant to standard DFT functionals such as the PBE functional, higher levels of theory must be used.

An often used approach to overcome these errors is to utilize hybrid functionals, which include a certain percentage of exact Fock exchange with the DFT exchange and correlation. Unfortunately, hybrid functionals are computationally very demanding and have in some cases been overlooked in favor of less computationally expensive methods, such as the "+*U*" correction,[95,96] or even a range of a posteriori corrections to LDA/GGA calculations.[97] Hybrid functionals often give better approximations of band gaps in semiconductor systems and provide improved structural data.[98] In this study, we have used the screened hybrid density functional developed by Heyd, Scuzeria, and Ernzerhof (HSE06),[99,100] as implemented in the VASP code.[101] Difficulties in evaluating the Fock exchange in a real space formalism are caused by the slow decay of the exchange interaction with distance. In the HSE06 hybrid functional approach, this problem is addressed by separating the description of the exchange interaction into long- and a short-range parts,[99] with a percentage (α = 25%) of exact nonlocal Fock exchange replacing the short-range (SR) PBE functional. A screening of ω = 0.11 bohr^{-1} is applied to partition the Coulomb potential into long-range (LR) and SR terms, which gives

$$E_{XC}^{HSE06}(\omega) = E_X^{HSE06,\,SR} + E_X^{PBE,\,LR} + E_C^{PBE} \quad (2)$$

where

$$E_X^{HSE06,\,SR} = \frac{1}{4}E_X^{Fock,\,SR} + \frac{3}{4}E_X^{PBE,\,SR} \quad (3)$$

Fock and PBE exchange are therefore only mixed in the SR part, with the LR exchange interactions being represented by the corresponding part of the range-separated PBE functional.[99] HSE06 has been shown to yield improved decriptions of structure, band gap, and defect properties of a number of oxide semiconductors.[102−116]

Structural optimizations of bulk CdO were performed using PBE and HSE06 at a series of volumes to calculate the equilibrium lattice parameters. In each case, the atomic positions, lattice vector, and cell angle were allowed to relax, while the total volume was held constant. The resulting energy volume curves were fitted to the Murnaghan equation of state to obtain the equilibrium bulk cell volume.[117] This approach minimizes the problems of Pulay stress and changes in basis set which can accompany volume changes in plane-wave calculations. The Pulay stress affects the stress tensor which is not used in obtaining the optimized lattice vectors, and hence this approach is significantly more accurate than using the stress tensor to perform constant pressure optimization. Convergence with respect to *k*-point sampling and plane-wave energy cut off were checked, and for both PBE and HSE06 a cutoff of 400 eV and a *k*-point sampling of $8 \times 8 \times 8$ were found to be sufficient. Calculations were deemed to be converged when the forces on all the atoms were less than 0.01 eV $Å^{-1}$.

As PBE produces a very poor description of the bulk electronic structure of CdO, we carried out all our defect calculations at the HSE06 level. A $2 \times 2 \times 2$ simulation cell consisting of 64 atoms was used for our defect calculations. The plane-wave cutoff was set at 400 eV, and a $2 \times 2 \times 2$ Monkhorst−Pack special *k*-point grid was used in all defect calculations. Structural optimizations were considered to be converged once the forces on all species were less than 0.02 eV $Å^{-1}$. All defect calculations were spin polarized. Density of states are shown with a Gaussian smearing of 0.02 eV.

The formation energy of a defect determines its equilibrium concentration. For defect D in charge state q, the formation energy is given by

$$\Delta H_f(D,q) = (E^{D,q} - E^{H}) + \sum_i n_i(E_i + \mu_i) + q(E_{Fermi} + \varepsilon^{H}_{VBM}) + E_{align}[q] \quad (4)$$

where E^{H} is the energy of the pure host supercell, and $E^{D,q}$ is the energy of the defective cell. E_i corresponds to elemental reference energies, i.e., $Cd_{(s)}$, $O_{2(g)}$, and $H_{2(g)}$; μ_i is the chemical potential of the species in question; and n is the number of atoms added to or taken from an external reservoir.[118] Electrons are exchanged with the Fermi level (E_F), which ranges from the VBM (E_F = 0 eV) to the calculated CBM. ε^{H}_{VBM} is the VBM eigenvalue of the host bulk, and $E_{align}[q]$ is a correction used to align the VBM of the bulk and the defective supercells and also to correct for finite-size effects in the calculations of charged defects, performed using the freely available SXDEFECTALIGN code.[119] These finite-size effect corrections are necessary as the charge introduced into a cell can cause a spurious interaction with its periodic image, which can affect the energetics.[119] An additional correction was made to account for band-filling effects[120,121] and is especially necessary in the case of materials like CdO where defect states occupy strongly dispersive bands.

The chemical potentials, μ_i, reflect the specific equilibrium growth conditions, within the global constraint of the calculated enthalpy of the host, in this case CdO: $\mu_{Cd} + \mu_O = \Delta H_f^{CdO} = -2.15$ eV. The lower limit for μ_O, which characterizes a Cd-*rich*/O-*poor* environment, is determined by the formation of metallic Cd: $\Delta\mu_{Cd} = 0$ eV; $\Delta\mu_O = -2.15$ eV. The upper limit for μ_O (Cd-*poor*/O-*rich* conditions) is governed by O_2 formation: $\Delta\mu_{Cd} = -2.15$ eV; $\Delta\mu_O = 0$ eV. We have also considered CdO_2 formation, but it was found to not be a chemical potential limit. Under both sets of conditions, the solubilities of H-related species are limited by the formation of H_2O, i.e., $\mu_O + 2\mu_H \leq \Delta H_f^{H_2O} = -2.67$ eV. The thermodynamic transition levels (ionization levels) of a given defect, $\varepsilon_D(q/q')$, correspond to the Fermi-level positions at which a given defect changes from charge state q to q'

$$\varepsilon_D(q/q') = \frac{\Delta H^f(D,q) - \Delta H^f(D,q')}{q' - q} \quad (5)$$

AUTHOR INFORMATION

Corresponding Author
scanloda@tcd.ie; watsong@tcd.ie

ACKNOWLEDGMENT

The authors thank P. D. C. King, L. F. J. Piper and A. Walsh for extremely useful discussions. This work was supported by SFI through the PI programme (PI Grant numbers 06/IN.1/I92 and 06/IN.1/I92/EC07). Calculations were performed on the IITAC, Lonsdale and Kelvin clusters as maintained by TCHPC and the Stokes cluster as maintained by ICHEC.

REFERENCES

(1) Thomas, G. *Nature* **1997**, *389*, 907.
(2) Ingram, B. J.; Gonzalez, G. B.; Kammler, D. R.; Bertoni, M. I.; Mason, T. O. *J. Electroceram.* **2004**, *13*, 167–175.
(3) Hayashi, K.; Matsuishi, S.; Kamiya, T.; Hirano, M.; Hosono, H. *Nature* **2002**, *419*, 462–465.
(4) Minami, T. *Semicond. Sci. Technol.* **2005**, *20*, S35–S44.
(5) Gordon, R. G. *MRS Bull.* **2000**, *25*, 52–57.
(6) Wang, L.; Matson, D. W.; Polikarpov, E.; Swensen, J. S.; Bonham, C. C.; Cosimbescu, L.; Berry, J. J.; Ginley, D. S.; Gaspar, D. J.; Padmaperuma, A. B. *J. Appl. Phys.* **2010**, *107*, 043103.
(7) Koffyberg, F. P. *Phys. Rev. B* **1976**, *13*, 4470.
(8) Jefferson, P. H.; Hatfield, S. A.; Veal, T. D.; King, P. D. C.; McConville, C. F.; Zúñiga Pérez, J.; Muñoz Sanjosé, V. *Appl. Phys. Lett.* **2008**, *92*, 022101–3.
(9) Vasheghani Fahrahani, S.; Veal, T. D.; King, P. D. C.; Zúñiga-Pérez, J.; Munoz-Sanjoé, V.; McConville, C. F. *J. Appl. Phys.* **2011**, *109*, 073712.
(10) Li, X.; Gessert, T. A.; Coutts, T. *Appl. Surf. Sci.* **2004**, *223*, 138–143.
(11) Wang, A.; Babcock, J. R.; Edleman, N. L.; Metz, A. W.; Lane, M. A.; Asahi, R.; Dravid, V. P.; Kannewurf, C. R.; Freeman, A. J.; Marks, T. J. *Proc. Natl. Acad. Sci. U.S.A.* **2001**, *98*, 7113–7116.
(12) Kammler, D. R.; Harder, B. J.; Hrabe, N. W.; McDonald, N. M.; Gonzalez, G. B.; Penake, D. A.; Mason, T. O. *J. Am. Ceram. Soc.* **2002**, *85*, 2345–2352.
(13) Cimino, A.; Marezio, M. *J. Phys. Chem. Solids* **1960**, *17*, 57–64.
(14) Gulino, A.; Tabbi, G. *Appl. Surf. Sci.* **2005**, *245*, 322–327.
(15) Haul, R.; Just, D. *J. Appl. Phys.* **1962**, *33*, 487–493.
(16) Ingram, B. J.; Gonzalez, G. B.; Kammler, D. R.; Bertoni, M. I.; Mason, T. O. *J. Electroceram.* **2004**, *13*, 167–175.
(17) Van de Walle, C. G. *Phys. Rev. Lett.* **2000**, *85*, 1012.
(18) Cox, S. F. J.; Lord, J. S.; Cottrell, S. P.; Gil, J. M.; Alberto, H. V.; Keren, A.; Prabhakaran, D.; Scheuermann, R.; Stoykov, A. *J. Phys.: Condens.Matter* **2006**, *18*, 1061–1078.
(19) Kilic, C.; Zunger, A. *Appl. Phys. Lett.* **2002**, *81*, 73–75.
(20) King, P. D. C.; Veal, T. D.; Jefferson, P. H.; Zúñiga Pérez, J.; Muñoz Sanjosé, V.; Mc-Conville, C. F. *Phys. Rev. B* **2009**, *79*, 035203–5.
(21) Clark, S. J.; Robertson, J.; Lany, S.; Zunger, A. *Phys. Rev. B* **2010**, *81*, 115311.
(22) Singh, A. K.; Janotti, A.; Scheffler, M.; Van de Walle, C. G. *Phys. Rev. Lett.* **2008**, *101*, 055502.
(23) Singh, H. P.; Dayal, B. *Solid State Commun.* **1969**, *7*, 725–726.
(24) Schleife, A.; Fuchs, F.; Furthmuller, J.; Bechstedt, F. *Phys. Rev. B* **2006**, *73*, 245212–14.
(25) Piper, L. F. J.; DeMasi, A.; Smith, K. E.; Schleife, A.; Fuchs, F.; Bechstedt, F.; Zuniga-Perez, J.; Munoz-Sanjose, V. *Phys. Rev. B* **2008**, *77*, 125204–4.

(26) King, P. D. C.; Veal, T. D.; Schleife, A.; Zuniga-Perez, J.; Martel, B.; Jefferson, P. H.; Fuchs, F.; Munoz-Sanjose, V.; Bechstedt, F.; McConville, C. F. *Phys. Rev. B* **2009**, *79*, 205205.
(27) Demchenko, I. N.; Denlinger, J. D.; Chernyshova, M.; Yu, K. M.; Speaks, D. T.; Olade-Velasco, P.; Hemmers, O.; Walukiewicz, W.; Derkachova, A.; Lawniczal-Jablonska, K. *Phys. Rev. B* **2010**, *82*, 075107.
(28) McGuinness, C.; Stagarescu, C. B.; Ryan, P. J.; Downes, J. E.; Fu, D.; Smith, K. E.; Egdell, R. G. *Phys. Rev. B* **2003**, *68*, 165104.
(29) Kılıç, Ç.; Zunger, A. *Phys. Rev. Lett.* **2002**, *88*, 095501.
(30) Nie, X. L.; Wei, S. H.; Zhang, S. B. *Phys. Rev. B* **2002**, *65*, 075111.
(31) Scanlon, D. O.; Watson, G. W. *Chem. Mater.* **2009**, *21*, 5435–5442.
(32) Schleife, A.; Rödl, C.; Fuchs, F.; Furthmüller, J.; Bechstedt, F. *Phys. Rev. B* **2009**, *80*, 035112–10.
(33) Varley, J. B.; Weber, J. R.; Janotti, A.; deWalle, C. G. V. *Appl. Phys. Lett.* **2010**, *97*, 142106.
(34) Lany, S.; Zunger, A. *Phys. Rev. Lett.* **2011**, *106*, 069601.
(35) King, P. D. C.; Lichti, R. L.; Celebi, Y. G.; Gil, M.; Vilao, R. C.; Alberto, H. V.; Piroto Duarte; Payne, D. J.; Egdell, R. G.; McKenzie, I.; McConville, C. F.; Cox, S. F. J.; Veal, T. D. *Phys. Rev. B* **2009**, *80*, 081201(R).
(36) Limpijumnong, S.; Reunchan, P.; Janotti, A.; Van de Walle, C. G. *Phys. Rev. B* **2009**, *80*, 193202.
(37) Janotti, A.; Van de Walle, C. G. *Nat. Mater.* **2007**, *6*, 44–47.
(38) King, P. D. C.; McKenzie, I.; Veal, T. D. *Appl. Phys. Lett.* **2010**, *96*, 062110.
(39) Robertson, J.; Clark, S. J. *Phys. Rev. B* **2011**, *83*, 075205.
(40) Zhu, Y. Z.; Chen, G. D.; Ye, H.; Walsh, A.; Moon, C. Y.; Wei, S. H. *Phys. Rev. B* **2008**, *77*, 245209.
(41) Zhang, S. B. *J. Phys.: Condens. Matter* **2002**, *14*, R881–R903.
(42) Janotti, A.; Van de Walle, C. G. *Phys. Rev. B* **2007**, *76*, 165202.
(43) Sokol, A. A.; French, S. A.; Bromley, S. T.; Catlow, C. R. A.; van Dam, H. J. J.; Sherwood, P. *Faraday Discuss.* **2007**, *134*, 267–282.
(44) Sokol, A. A.; Walsh, A.; Catlow, C. R. A. *Chem. Phys. Lett.* **2010**, *492*, 44–48.
(45) Godinho, K. G.; Walsh, A.; Watson, G. W. *J. Phys. Chem. C* **2009**, *113*, 439–448.
(46) Agoston, P.; Korber, C.; Klein, A.; Puska, M. J.; Nieminen, R. M.; Albe, K. *J. Appl. Phys.* **2010**, *108*, 053511.
(47) Hoffman, C. W. W.; Ropp, R. C.; Mooney, R. W. *J. Am. Chem. Soc.* **1959**, *81*, 3830–3834.
(48) Walukiewicz, W. *Appl. Phys. Lett.* **1989**, *54*, 2094.
(49) Speaks, D. T.; Mayer, M. A.; Yu, K. M.; Mao, S. S.; Haller, E. E.; Walukiewicz, W. *J. Appl. Phys.* **2010**, *107*, 113706.
(50) Walsh, A.; Silva, J. L. F. D.; Wei, S.-H. *Phys. Rev. B* **2008**, *78*, 075211.
(51) King, P. D. C.; Veal, T. D.; McConville, C. F.; Zúñiga-Pérez, J.; Muñoz-Sanjosé, V.; Hopkinson, M.; Rienks, E. D. L.; Fulsang Jensen, M.; Hofmann, P. *Phys. Rev. Lett.* **2010**, *104*, 256803.
(52) Piper, L. F. J.; Colakerol, L.; King, P. D. C.; Schleife, A.; Zuniga-Perez, J.; Glans, P.-A.; Learmonth, T.; Federov, A.; Veal, T. D.; Fuchs, F.; Munoz-Sanjose, V.; Bechstedt, F.; McConville, C. F.; Smith, K. E. *Phys. Rev. B* **2008**, *78*, 165127–5.
(53) Piper, L. F. J.; Jefferson, P. H.; Veal, T. D.; McConville, C. F.; Zuniga-Perez, J.; Munoz-Sanjose, V. *Superlattices Microstruct.* **2007**, *42*, 197–200.
(54) Yang, Y.; Jin, S.; Medvedeva, J. E.; Ireland, J. R.; Metz, A. W.; Ni, J.; Hersam, M. C.; Freeman, A. J.; Marks, T. J. *J. Am. Chem. Soc.* **2005**, *127*, 8796–8804.
(55) Jin, S.; Yang, Y.; Medvedeva, J. E.; Ireland, J. R.; Metz, A. W.; Ni, J.; Kannewurf, C. R.; Freeman, A. J.; Marks, T. J. *J. Am. Chem. Soc.* **2004**, *126*, 13787–12793.
(56) Lany, S.; Zunger, A. *Phys. Rev. B* **2008**, *78*, 235104.
(57) Janotti, A.; Van de Walle, C. G. *Appl. Phys. Lett.* **2005**, *87*, 122102.
(58) Oba, F.; Togo, A.; Tanaka, I.; Paier, J.; Kresse, G. *Phys. Rev. B* **2008**, *77*, 245202.
(59) Lany, S.; Zunger, A. *Phys. Rev. B* **2010**, *81*, 113201.
(60) Agoston, P.; Albe, K.; Nieminen, R. M.; Piska, M. J. *Phys. Rev. Lett.* **2009**, *103*, 245501.
(61) Janotti, A.; Van de Walle, C. G. *Phys. Rev. B* **2007**, *76*, 165202.
(62) Bader, R. F.W. *Atoms inMolecules: A Quantum Theory*; International series of monographs on chemistry; Oxford University Press: Oxford, 1990.
(63) Kehoe, A. B.; Scanlon, D. O.; Watson, G. W. *Phys. Rev. B* **2011**, *83*, 233202.
(64) Walukiewicz, W. *J. Cryst. Growth* **1996**, *159*, 244–247.
(65) Walukiewicz, W. *Phys. B. Condens. Matter* **2001**, *302−303*, 123–134.
(66) Zhang, S. B.; Wei, S. H.; Zunger, A. *J. Appl. Phys.* **1998**, *83*, 3192.
(67) Zhang, S. B.; Wei, S. H.; Zunger, A. *Phys. Rev. Lett.* **2000**, *84*, 1231–1235.
(68) Hosono, H.; Ogo, Y.; Yanagi, H.; Kamiya, T. *Electrochem. Solid State Lett.* **2011**, *14*, H13–H16.
(69) Schleife, A.; Fuchs, F.; Rodl, C.; Furthmuller, J.; Bechstedt, F. *Appl. Phys. Lett.* **2009**, *94*, 012104.
(70) Hoffling, B.; Schleife, A.; Fuchs, F.; Rodl, C.; Bechstedt, F. *Appl. Phys. Lett.* **2010**, *97*, 032116.
(71) Asahi, R.; Wang, A.; Babcock, J. R.; Edleman, N. L.; Metz, A. W.; Lane, M. A.; Dravid, V. P.; Kannewurf, C. R.; Freeman, A. J.; Marks, T. J. *Thin Solid Films* **2002**, *411*, 101–105.
(72) Zhao, Z.; Morel, D. L.; Ferekides, C. S. *Thin Solid Films* **2002**, *413*, 203–211.
(73) Yan, M.; Lane, M.; Kannewurf, C. R.; Chang, R. P. H. *Appl. Phys. Lett.* **2001**, *78*, 2342–2344.
(74) Vigil, O.; Cruz, F.; Morales-Acevedo, A.; Contreras-Puente, G.; Vaillant, L.; Santana, G. *Mater. Chem. Phys.* **2001**, *68*, 249–252.
(75) Ueda, N.; Maeda, H.; Hosono, H.; Kawazoe, H. *J. Appl. Phys.* **1998**, *84*, 6174–6177.
(76) Saha, B.; Thapa, R.; Chattopadhyay, K. *Solid State Commun.* **2008**, *145*, 33–37.
(77) Piper, L. F. J.; Veal, T. D.; Mahboob, I.; McConville, C. F.; Lu, H.; Schaff, W. J. *Phys. Rev. B* **2004**, *70*, 115333.
(78) Piper, L. F. J.; Veal, T. D.; McConville, C. F.; Lu, H.; Schaff, W. J. *Phys. Status Solidi C* **2006**, *3*, 1841–1845.
(79) King, P. D. C.; Veal, T. D.; Jefferson, P. H.; Hatfield, S. A.; Piper, L. F. J.; McConville, C. F.; Fuchs, F.; J., F.; Bechstedt, F.; Lu, H.; Schaff, W. J. *Phys. Rev. B* **2008**, *77*, 045316.
(80) Colakerol, L.; et al. *Phys. Rev. Lett.* **2006**, *97*, 237601.
(81) Mahboob, I.; D., V. T.; Piper, L. F. J.; McConville, C. F.; Lu, H.; Schaff, W. J.; Furthmüller, J.; Bechstedt, F. *Phys. Rev. B* **2004**, *69*, 201307(R).
(82) King, P. D. C.; et al. *Appl. Phys. Lett.* **2007**, *91*, 092101.
(83) Linhart, W. M.; Veal, T. D.; King, P. D. C.; Koblmuller, G.; Gallinat, C. S.; Speck, J. S.; McConville, C. F. *Appl. Phys. Lett.* **2010**, *97*, 112103.
(84) Piper, L. F. J.; Veal, T. D.; Lowe, M. J.; McConville, C. F. *Phys. Rev. B* **2006**, *73*, 195321.
(85) Weber, J. R.; Janotti, A.; Van de Walle, C. G. *Appl. Phys. Lett.* **2010**, *97*, 192106.
(86) Olsson, L. O.; Andersson, C. M. M.; Hakansson, M. C.; Kanski, J.; Ilver, U. O.; Karlsson, L. *Phys. Rev. Lett.* **1996**, *76*, 3626.
(87) King, P. D. C.; Veal, T. D.; Payne, D. J.; Bourlange, A.; Egdell, R. G.; McConville, C. F. *Phys. Rev. Lett.* **2008**, *101*, 116808.
(88) King, P. D. C.; Veal, T. D.; FUchs, F.; Wang, C. Y.; Payne, D. J.; Bourlange, A.; Zhang, H.; Bell, G. R.; Cimalla, V.; Ambacher, O.; Egdell, R. G.; Bechstedt, F.; McConville, C. F. *Phys. Rev. B* **2009**, *79*, 205211.
(89) Walsh, A.; Da Silva, J. L. F.; Wei, S. H.; Korber, C.; Klein, A.; Piper, L. F. J.; DeMasi, A.; Smith, K. E.; Panaccione, G.; Torelli, P.; Payne, D. J.; Bourlange, A.; Egdell, R. G. *Phys. Rev. Lett.* **2008**, *100*, 167402.
(90) Kresse, G.; Furthmüller, J. *Phys. Rev. B* **1996**, *54*, 11169–11186.
(91) Kresse, G.; Hafner, J. *Phys. Rev. B* **1994**, *49*, 14251–14271.
(92) Perdew, J. P.; Burke, K.; Ernzerhof, M. *Phys. Rev. Lett.* **1996**, *77*, 3865.
(93) Blöchl, P. E. *Phys. Rev. B* **1994**, *50*, 17953.
(94) Kresse, G.; Joubert, D. *Phys. Rev. B* **1999**, *59*, 1758–1775.
(95) Dudarev, S. L.; Botton, G. A.; Savrasov, S. Y.; Humphreys, C. J.; Sutton, A. P. *Phys. Rev. B* **1998**, *57*, 1505.

(96) Morgan, B. J.; Scanlon, D. O.; Watson, G. W. *e-J. Surf. Sci. Nano Technol.* **2009**, *7*, 395–404.
(97) Raebiger, H.; Lany, S.; Zunger, A. *Phys. Rev. B* **2007**, *76*, 045209.
(98) Labat, F.; Baranek, P.; Domain, C.; Minot, C.; Adamo, C. *J. Chem. Phys.* **2007**, *126*, 154703.
(99) Heyd, S.; Scuseria, G. E.; Ernzerhof, M. *J. Chem. Phys.* **2003**, *118*, 8207–8215.
(100) Krukau, A. V.; Vydrov, O. A.; Izmaylov, A. F.; Scuseria, G. E. *J. Chem. Phys.* **2006**, *125*, 224106.
(101) Paier, J.; Marsman, M.; Hummer, K.; Kresse, G.; Gerber, I. C.; Ángyán, J. G. *J. Chem. Phys.* **2006**, *124*, 154709–154713.
(102) Heyd, J.; Scuseria, G. E. *J. Chem. Phys.* **2004**, *121*, 1187–1192.
(103) Heyd, J.; Peralta, J. E.; Scuseria, G. E.; Martin, R. L. *J. Chem. Phys.* **2005**, *123*, 174101.
(104) Da Silva, J. L. F.; Ganduglia-Pirovano, M. V.; Sauer, J.; Bayer, V.; Kresse, G. *Phys. Rev. B* **2007**, *75*, 045121.
(105) Walsh, A.; Da Silva, J. L. F.; Yan, Y.; Al-Jassim, M. M.; Wei, S. H. *Phys. Rev. B* **2009**, *79*, 073105.
(106) Chen, S.; Gong, Z. G.; Walsh, A.; Wei, S. H. *Appl. Phys. Lett.* **2009**, *94*, 041903.
(107) Allen, J. P.; Scanlon, D. O.; Watson, G. W. *Phys. Rev. B* **2010**, *81*, 161103(R).
(108) Scanlon, D. O.; Watson, G. W. *J. Phys. Chem. Lett.* **2010**, *1*, 3195–3199.
(109) Janesko, B. G.; Henderson, T. M.; Scuseria, G. E. *Phys. Chem. Chem. Phys.* **2009**, *11*, 443–454.
(110) Scanlon, D. O.; Watson, G. W. *J. Phys. Chem. Lett.* **2010**, *1*, 2582–2585.
(111) Peralta, J. E.; Heyd, J.; Scuseria, G. E.; Martin, R. L. *Phys. Rev. B* **2006**, *74*, 073101.
(112) Scanlon, D. O.; Morgan, B. J.; Watson, G. W.; Walsh, A. *Phys. Rev. Lett.* **2009**, *103*, 096405.
(113) Stroppa, A.; Kresse, G. *Phys. Rev. B* **2009**, *79*, 201201(R).
(114) Stroppa, A.; Picozzi, S. *Phys. Chem. Chem. Phys.* **2010**, *12*, 5405–5416.
(115) Scanlon, D. O.; Watson, G. W. *J. Mater. Chem.* **2011**, *21*, 3655.
(116) Scanlon, D. O.; Watson, G. W. *Phys. Rev. Lett.* **2011**, *106*, 186403.
(117) Murnaghan, F. D. *Proc. Natl. Acad. Sci. U.S.A.* **1944**, *30*, 244–247.
(118) Van de Walle, C. G.; Neugebauer, J. *J. Appl. Phys.* **2004**, *95*, 3851–3879.
(119) Freysoldt, C.; Neugebauer, J.; de Walle, C. G. V. *Phys. Rev. Lett.* **2009**, *102*, 016402.
(120) Lany, S.; Zunger, A. *Phys. Rev. B* **2008**, *78*, 235104.
(121) Walsh, A.; Yan, Y. F.; Al-Jassim, M. M.; Wei, S. H. *J. Phys. Chem. C* **2008**, *112*, 12044.